Fe−Catecholate and Fe−Oxalate Vibrations and Isotopic Substitution Shifts from DFT Quantum Chemistry

Lars Öhrström*,† and Isabelle Michaud-Soret‡

Institutionen för Oorganisk kemi, Chalmers Tekniska Högskola, SE-412 96 Göteborg, Sweden, and CEA/Département de Recherche Fondamentale sur la Matière Condensée, Service de Chimie Inorganique et Biologique, Laboratoire de Chimie de Coordination (Unité de Recherche Associée au CNRS No 1194), CEA-Grenoble, F-38054 Grenoble cedex 9, France

Received: March 16, 1998; In Final Form: October 22, 1998

Quantum chemical model calculations using density functional theory (DFT) were used to assign iron−catecholate and iron−oxalate vibrations and to get quantitative predictions of the isotopic shifts. Full geometry optimizations and vibrational analyses were performed for catechol, Fe(catecholate)$^{2-}$, Fe(4-methyl-catecholate)$^{2-}$, [Fe(oxalate)$_3$]$^{3-}$, and Fe(oxalate)$^{2-}$. The advantages of Fe(0) versus Fe(III) models are discussed. For selected systems $^{16/18}$O, $^{54/57}$Fe, and $^{1/2}$H isotopic substitution shifts are reported. They were successfully matched to experimental patterns from recent resonance Raman studies of tyrosine hydroxylase and allowed more precise assignments of the observed bands. The nature of the catecholate C═O and Fe−O vibrations were clarified, and the existence of a chelate vibration mode was confirmed. A band predicted at ∼320 cm^{-1} was assigned to a new νFe−O vibration with a large $^{54/57}$Fe isotope effect, and no significant $^{54/57}$Fe shifts were observed for the other Fe−O vibrations. We note that with the commonly used diatomic harmonic oscillator model one can only make a rough estimation of these shifts. DFT model calculations are suggested as a more precise tool when interpreting isotopic substitution shifts in vibrational spectra.

Introduction

In the studies of metal complexes, a very wide selection of experimental techniques is normally available for any chosen molecule. IR spectra can, for example, routinely be supported by X-ray diffraction and multinuclear NMR spectroscopy. However, this is not the case for metalloproteins, where the choice of method is more limited and the signal-to-noise ratio generally is lower. In this field, it is therefore essential to extract maximum information from the technique applied in each case.

Vibrational spectroscopies[1−3] and especially the resonance Raman technique[4−8] are important tools in the studies of metalloproteins. Often isotopic labeling is used to help assign spectra and, consequently, to interpret the metal environment. In this context, it is clear that a precise prediction of the isotopic shifts for competing metal site models may be useful. Although these shifts can be calculated after a complete normal coordinate analysis of the spectrum, such an analysis is not always possible. Then, one has to rely on the diatomic harmonic oscillator for a rough estimation of the shifts, but this model has obvious shortcomings since it cannot take into account the true nature of the vibrations.[1]

An alternative would be to calculate the isotopic shifts with some theoretical method. Density functional theory is now becoming increasingly popular for the calculation of vibrational frequencies, especially for organic molecules.[9,10] DFT[11] has the advantage of being as fast or faster than conventional Hartree−Fock methods but at the same time including correlation effects. Also, several studies with vibrational analysis of transition metal complexes have been published.[12−15] We have recently reported preliminary data of our DFT calculations on catechol and Fe(catecholate)$^{2-}$ [16] and showed how these model calculations matched experimental isotopic shifts from a study of catecholate complexes to the Fe(III) site in tyrosine hydroxylase[6] within a few wavenumbers, thereby confirming the proposed coordination mode of the catecholate derivatives.

The particular interest in these calculations stems from the use of catecholate-type ligands as spectroscopic probes for nonheme iron proteins.[6,17−26] Derivatives of catechol also play an important biological role; an example is the above-mentioned enzyme tyrosine hydroxylase that catalyzes the rate-limiting step in the biosynthesis of catecholamines such as 3,4-dihydroxyphenyl ethylamine, dopamine. Our purpose is to predict isotopic substitution shifts from vibrational spectra of iron−catecholate complexes by the use of calculations on simple model compounds. In this article, we report the full geometry optimizations and vibrational analyses by DFT for catechol, Fe(catecholate)$^{2-}$, Fe(4-methyl-catecholate)$^{2-}$, [Fe(oxalate)$_3$]$^{3-}$, and Fe(oxalate)$^{2-}$ as well as the $^{16/18}$O and $^{54/57}$Fe isotopic substitution shifts (Scheme 1). The smaller Fe(0) models are compared to larger, more realistic Fe(III) molecules, and the scope and limitations of the Fe(0) models are discussed.

Computational Details. Full geometry optimizations and vibrational analyses were performed for catechol, Fe(catecholate)$^{2-}$, Fe(4-methyl-catecholate)$^{2-}$, [Fe(oxalate)$_3$]$^{3-}$, Li$_3$[Fe(oxalate)$_3$] (no vibrational analysis), and Fe(oxalate)$^{2-}$ using the DGauss 2.3 and 3.0 DFT program,[27] included in the UniChem package.[28] Fixed geometry calculations were carried out for [Fe(catecholate)(oxalate)$_2$]$^{3-}$ using the optimized geometry for [Fe(oxalate)$_3$]$^{3-}$ with one oxalate replaced by catecholate using the Fe(catecholate)$^{2-}$ geometry. At the local spin density level (referred to as LSD calculations), the VWN functional was used.[29a] For the nonlocal corrections to the exchange-correlation

* Corresponding author. E-mail: ohrstrom@inoc.chalmers.se. Phone: +46 31 772 28 71. Fax: +46 31 772 28 46.
† Chalmers Tekniska Högskola.
‡ CEA.

10.1021/jp981508f CCC: $18.00
Published on Web 01/14/1999

SCHEME 1

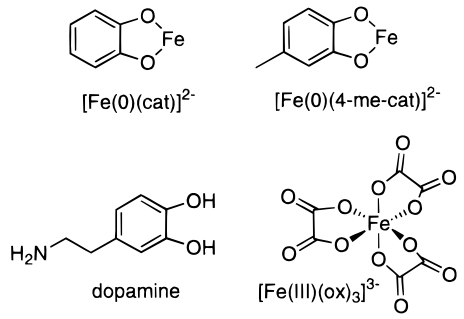

energy, the Becke−Perdew functional, including a gradient corrected exchange, was applied self-consistently (referred to as BP calculations).[29b−c] BP calculations were used on the catechol and the Fe(0) complexes since this method, although somewhat more costly, should in principle give better results. However, for the larger $[Fe(oxalate)_3]^{3-}$ models, the LSD level was used in order to minimize the computational effort.[30] Reference calculations on $Fe(oxalate)^{2-}$ showed that in this case the methods gave essentially the same vibrational modes.

A double-ζ split-valence plus polarization basis set optimized for DFT calculations, DZVP, was used.[31] The contracted basis sets had the following composition: H [2s], C, N, O [3s,2p,1d], Li [3s,1p,1d], Fe [5s,3p,2d].

The geometry optimizations and the vibrational analyses were made by analytical determinations of the first and second derivatives of the total energy. No symmetry constraints were used.

The calculations on the Fe(0) complexes were made on the $S = 0$ state in a spin-restricted manner. We note that this closed-shell singlet may not be the ground state for these molecules. Calculations on $Fe(oxalate)^{2-}$ show the $S = 1$ state to be lower in energy by about 1 kcal/mol and the $S = 2$ state to be lower by another 9 kcal/mol. The effects on the vibrational frequencies are small, except for Fe−O modes; for example, the δ,νFe−O mode at 548 cm^{-1} is lowered to 503 cm^{-1} and then further to 467 cm^{-1}.[32]

For the Fe(III) complexes, we used the $S = 5/2$ spin state, which is the experimentally verified spin state for $[Fe(oxalate)_3]^{3-}$.[33] For the Fe(0) models, the geometry optimization gradient convergence threshold was 8×10^{-4} bohr/Å ("medium") and the numerical grid for the exchange-correlation was set at the "medium" level. To obtain the correct symmetry for the Fe(III) complexes, for example all Fe−O bonds equal, it was necessary to set the gradient convergence threshold to 5×10^{-4} bohr/Å ("tight") and the numerical grid for the exchange-correlation to "fine".

Results and Discussion

We will present our results in the following way. First, we discuss the geometry and frequencies for catechol, Fe(catecholate)$^{2-}$, and Fe(4-methyl-catecholate)$^{2-}$. Then, we show that the Fe(0) models give results in line with Fe(III) complexes by comparing our results for $[Fe(oxalate)_3]^{3-}$ and $Fe(oxalate)^{2-}$. Finally, we discuss the isotopic substitution shifts, the experimental quantity of most interest to us. We note here that we will then compare *differences* between calculated values with experiment, a procedure more likely to be successful than the comparison of *absolute* calculated values with experiment.

Catechol. BP DFT calculations on free catechol gave a geometry (Figure 1) and frequencies in reasonable agreement with experimental data,[34−38] as expected in view of recent results on related phenoxy systems.[39,40] The C−C bond lengths are too

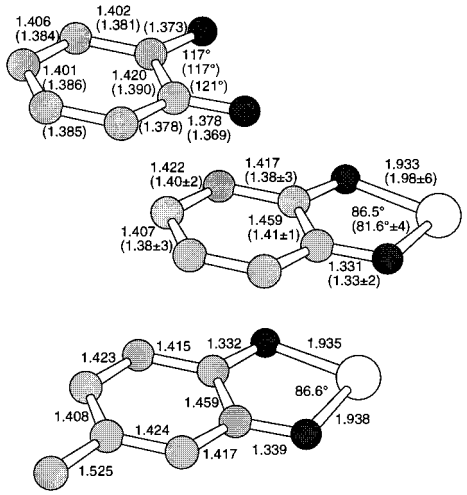

Figure 1. Optimized geometries [Å] for catechol, Fe(catecholate)$^{2-}$, and Fe(4-methyl-catecholate)$^{2-}$. Experimental values [Å] are from ref 34 (catechol) and ref 42−46 (average values for Fe(III)catecholate complexes with the variation between different complexes added as ± in parentheses). Hydrogen atoms are omitted for clarity.

long by in average 0.02 Å compared to the X-ray crystal structure of catechol[34a] but agree better with the vapor-phase data from microwave spectroscopy.[34b] A major difference between the calculated structure and the X-ray structure is the hydrogen bond network present in the solid state. This causes the OH groups to adopt different conformations so that the solid-state catechol geometry is no longer C_{2v} symmetric and, furthermore, the molecule is not perfectly planar. Also, in the gas phase the molecule is C_s symmetric,[34b] but in polar solvents such as water, it adopts the C_{2v} structure.[38] Usually, the idealized C_{2v} structure is used in the vibrational analysis,[37] but detailed studies of the C_s to C_{2v} conversion and its effect on the vibrational spectra have recently been performed.[38]

There is no complete consensus in the literature on the vibration modes in the experimental spectra,[37,38] and our frequencies and assignments based on the C_{2v} structure are found in Table 1. For the O−H and C−H stretching vibrations, the error is around 50 cm^{-1}, but between 1600 and 700 cm^{-1}, where there are vapor data available, the error improves to an average of 11 cm^{-1}. The discrepancy of the symmetry assignments of some modes in ref 37a,b may be due to the two possible arrangements of the coordinate axes in substituted benzenes with C_{2v} symmetry.

One should note, though, that the assignment of experimental signals based on calculated frequencies only is not advisable when the vibrations are of the same type and fall within 0−40 cm^{-1}. However, when data for deuterated samples are available, as in ref 37b, we can make more reliable assignments based on the calculated frequencies and isotopic shifts. For example, the difference between the 8a and 8b vibrations (Table 1) is only 16 cm^{-1} (exptl 9 cm^{-1}), but these vibrations have close calculated and experimental frequency shifts on deuteration (33 and 21 cm^{-1} calculated versus the observed 31 and 17 cm^{-1}), thus confirming the assignment. For many of the δCH vibrations, the modes are different for the catechol-d_6 and we cannot say that one particular line has moved to a new position, so the shifts in Table 1 are somewhat arbitrary for these vibrations.

The largest discrepancies come for the symmetric ring stretch. The observed frequencies agree within 17 cm^{-1}, but the measured deuteration shift in the vapor phase is only 39 cm^{-1}, compared to the calculated 68 cm^{-1}. In the solid state, however, the same shift is 57 cm^{-1}.[37a]

TABLE 1: Experimental and Calculated Vibrational Frequencies for Catechol and the Catechol-d_6 Isotopic Substitution Shifts

experiment[a]			calculation, DFT-BP		
ν/cm^{-1}	$\Delta\nu_{H-D}$/cm^{-1}	assignment[d,e]	ν/cm^{-1}	$\Delta\nu_{H-D}$/cm^{-1}	assignment[f]
3663	1041	νOH, A_1	3659	986	νOH
3605	1039	νOH, B_2	3653	985	νOH
3069	673	νCH, A_1, 20a	3145	808	νCH, A_1, 2
3063	744	νCH, A_1, 2	3130	810	νCH, B_2, 20a
3060	760	νCH, B_2, 7b	3106	806	νCH, 7b $\pm$ 20b
3051	747	νCH, B_2, 20b	3103	806	νCH, 7b $\pm$ 20b
1616	31	νCC, A_1, 8a	1618	33	νCC, A_1, 8a
1607	17	νCC + νCO, B_2, 8b	1602	21	νCC + νCO, B_2, 8b
1504	71	νCC + δCH, B_2, 14	1504	62	νCC + δCH, B_1, 19b
1479	75	νCC + νCO, B_2, 19b	1459	92	νCC + νCO, B_2, 19a
1365[b]	na	νCC, A_1, 14	1374	30	νCC, A_1, 14
1324	414	δOH, A_1	1332	283	δOH, B_2
1275	64[g]	νCO, A_1, 7a	1267	71[h]	νCO + δCH, A_1, 7a
1251	100	νCO, B_2, 7b	1248	56[h]	νCO + δCH, B_2, 3
1195	290[g]	δOH, B_2	1182	260	δOH, A_1
1151	221	δCH, A_1, 9a	1142	258[h]	δCH + δOH, B_2, 18a
1151	na	δOH, B_2	1129	260[h]	δCH + δOH, A_1, 9a
1092	214	δCH, B_2, 9b	1073	236[h]	δCH + δOH, B_2, 13
1035	168	δCH, A_1, 18a	1020	219[h]	δCH, A_1, 18b
916	163	γCH, B_2, 10b	900	166	γCH, A_2, 5
860[c]	110	γCH, B_2, 10b	841	74[h]	δCCC, B_2, 12
859	na	γCH, B_1, 17b	800	132	γCH, B_1, 17b
768	39	ring, A_1, 1	751	68	ring, A_1, 1
741	na	γCH, B_1, 11	741	39	δCCC, A_2, 17a
708[b]	108	δCCC, A_1, 12	676	128	δCCC + γCH, A_2, 4
582[c]	−4	δCCC, A_2, 16a	656	121	γCH, B_1, 11
564[b]	−4	δCCC, A_1, 10	572	21	δCCC, A_1, 6a
544[b]	−12	γCO, B_1, 20	549	68	δCCC, A_2, 16a
			524	18	ring, B_2, 6b
			430	40	νCC,B_2, 9b
			408	65	δCCC, B_1, 16b
445[b]	95	γOH, B_1	378	87	γOH, B_1
348[c]	na	γOH, B_1	322	61	γOH, A_2
287[b]	15	δCCC, A_1, 11	302	15	δCO + δOH, A_1, 15
215[b]	na	δCCC, B_1, 16b	268	45	δCCC, B_1, 10a
204[c]	na	δCCC, A_2, 16	166	12	δCCC, A_2, 10b

[a] Vapor data[37] except when otherwise noted. [b] Solution data.[37b] [c] Solid state.[37b] [d] Description, symmetry assignment, Wilson number. [e] Includes reassignments of ref 37a in ref 37b. [f] The DFT vibrations have assignments according to Varsányi.[35,36] [g] Raman solution. [h] The normal modes for the deuterated molecules are somewhat different.

TABLE 2: Mulliken Population Analysis for LSD Calculations on Fe(catecholate)$^{2-}$, [Fe(cat)(oxalate)$_2$]$^{3-}$, Fe(oxalate)$^{2-}$, [Fe(oxalate)$_3$]$^{3-}$, Li$_3$[Fe(ox)$_3$], and Catechol

population analysis	Fe(cat)$^{2-}$	[Fe(cat)(ox)$_2$]$^{3-}$[a]	Fe(ox)$^{2-}$	[Fe(ox)$_3$]$^{3-}$	Li$_3$[Fe(ox)$_3$]	H$_2$cat
atomic charges Fe	−0.74	0.60	−0.63	0.66	0.82	
O1	−0.54	−0.44	−0.44	−0.33	−0.35	−0.47
O2[b]			−0.44	−0.39	−0.50	
C1	0.31	0.29				0.23
C3	−0.40	−0.44				−0.36
C4	−0.28	−0.28	0.20	0.12	0.34	−0.25
overlap Fe−O	0.25	0.39	0.23	0.37	0.34	
ligand total charge	−1.26	−1.08	−1.37	−1.20	−1.01	−0.84[c]

[a] Charges for catecholate. [b] Noncoordinated oxygen. [c] Excluding hydroxyl protons.

Fe(catecholate)$^{2-}$ and Fe(4-methylcatecholate)$^{2-}$. To model the iron−catecholate bonding we used Fe(catecholate)$^{2-}$, and as a model for the biologically relevant 4-substituted catecholates, i.e., dopamine, we used Fe(4-methylcatecholate)$^{2-}$. The results from the geometry optimizations are shown in Figure 1, and some results from the population analysis are given in Table 2.

These Fe(0) models[41] may seem very electron rich compared to an Fe(III) system. However, one could argue that things are not this straightforward. If we do an electron count according to the 18-electron rule, an ordinary Fe(III)L$_6$ complex contains $5 + 2 \times 6 = 17$ electrons and the Fe(catecholate)$^{2-}$ model compound has $8 + 2 \times 2 = 12$ electrons.

The geometries are in reasonable agreement with experimental data[42−46] (see Figure 1) if we consider that we are comparing a model complex to a whole class of compounds. For example, different trans ligands and distortions from ideal octahedral coordination may have relatively large effects on the Fe−O distances, as indicated by the span of the experimental data, 1.92−2.04 Å.

We can compare the population analysis for the Fe(0) models with those of the Fe(III) compounds, Table 2. We note that the total charge of the catecholate ligand is higher (more negative) for Fe(catecholate)$^{2-}$ than for [Fe(cat)(ox)$_2$]$^{3-}$ but that this difference is relatively small (17%). The same observation can be made for the difference between [Fe(oxalate)$_3$]$^{3-}$ and Fe(oxalate)$^{2-}$ (14%). The total charge of the complex and also the nature of the auxiliary ligands may be decisive; calculations on the positively charged model compound [Fe(catecholate)-(NH$_3$)$_2$(H$_2$O)$_2$]$^{+}$ gave considerably lower charge on the cat-

TABLE 3: Fe(catecholate)$^{2-}$ and Fe(4-methylcatecholate)$^{2-}$ Frequencies Calculated by DFT[c]

calculation, DFT-BP		experimental,	DFT-BP,	experimental,
Fe(cat)$^{2-}$ (ν/cm^{-1})	assignment,[a] Fe(cat)$^{2-}$	TH-cat[b] (ν/cm^{-1})	Fe(4mecat)$^{2-}$ (ν/cm^{-1})	TH-dopamine[b] (ν/cm^{-1})
1540	νCC + νCO, B_2, 8b		1553	
1537	νCC, A_1, 8a	1566	1534	
1494	νCC + δCH, A_1, 19b	1466	1497	1475
1419	νCC + νCO, B_2, 19a		1398	1425
1351	νCC, A_1, 14	1314	1347	1316
1292	δCH + νCO, A_1, 7a	1257	1293	1275
1280	δCH + νCO, B_2, 3		1275	
1207	δCH, B_2		1209	
1116	δCH, A_1, 9a	1150	1140	
1065	δCH, B_2, 18a		1091	
1005	δCH, A_1, 18b		930	
862	δCCC, B_2, 12			
761	ring, A_1		784	
599	νFe−O, B_2, 9b		625	631
583	νFe−O, A_1, 15	619	552	592
502	ring, B_2, 6b			
489	δ,ν chelate, A_1	528	500	528
283	νFe−cat, A_1		282	
273	δFe−O, B2		230	

[a] Description, symmetry assignment, Wilson number. [b] Reference 6. [c] In the tables, ν indicates stretching and δ in-plane bending vibration modes. Only frequencies under 1600 cm^{-1} and in plane A_1, B_2 (cat), or a′ (4mecat) vibrations are reported. The calculations are compared to experimental data for tyrosine hydroxylase Fe(III) complexes with catecholate and dopamine. See Figure 2 for a more detailed description of some of the vibrations.

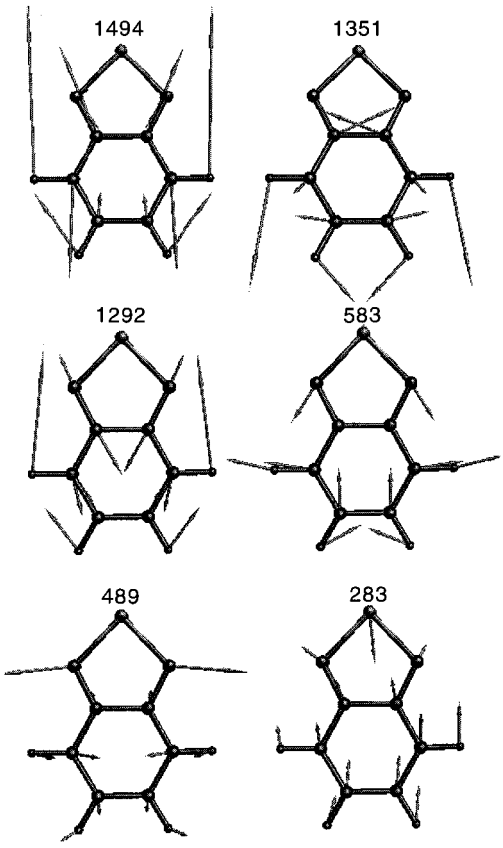

Figure 2. Atomic displacements of selected normal modes for Fe(catecholate)$^{2-}$ calculated by DFT. The scale of the displacements is arbitrary but common to all the modes.

echolate ligand, −0.35.[16] In this respect, one should remember that the biologically relevant ligands in this case are, for example, histidines, neutral N donors, and carboxylates, hydroxyls, and tyrosines, negative O donors. An important conclusion is that the catecholate has not been oxidized to a quinone or semiquinone.

The main advantage is that these models let us do some very rapid and inexpensive evaluations of vibrational frequencies.

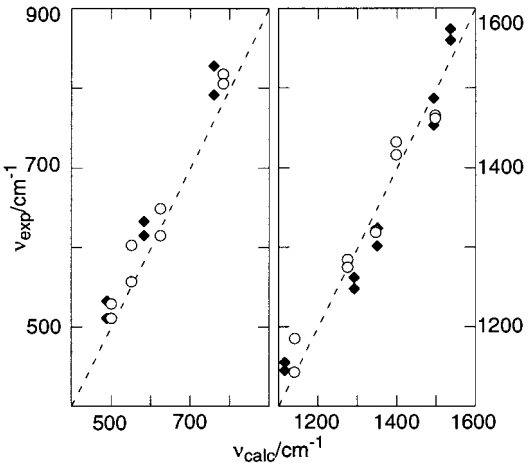

Figure 3. Upper and lower limits for experimental frequencies from six Fe(III)catecholate complexes (◆)[6,17a] and three different Fe(III) complexes with 4-substitution (○),[25] plotted as a function of the calculated values for Fe(catecholate)$^{2-}$ and Fe(4-methylcatecholate)$^{2-}$. The dashed lines correspond to a perfect agreement between theory and experiment. (The compounds in question are listed in notes 17a and 25.)

Calculated frequencies for the Fe−catecholate unit are reported in Table 3 together with experimental data from tyrosine hydroxylase Fe(III) catecholate complexes,[6] and some important normal modes are illustrated in Figure 2. In Figure 3, upper and lower limits for experimental frequencies from six Fe(III)-catecholate complexes[6,17a] and three different Fe(III)catecholate complexes with 4-substitution[25] have been plotted as a function of the calculated values.

A frequency unique to chelating catechol complexes, observed around 530 cm^{-1}, has been assigned to a mode intrinsic to the five-membered ring in analogy with iron−oxalate complexes.[17a] A notable result of our calculations is the confirmation of this "chelate"-type vibrational mode, calculated at 489 cm^{-1}; see Figure 2. It consists of a mixture of Fe−O stretching and bending modes, and we have consequently labeled it "δ,ν chelate". Note the close resemblance between this vibration and the 510 cm^{-1} [Fe(oxalate)$_3$]$^{3-}$ vibration in Figure 4.

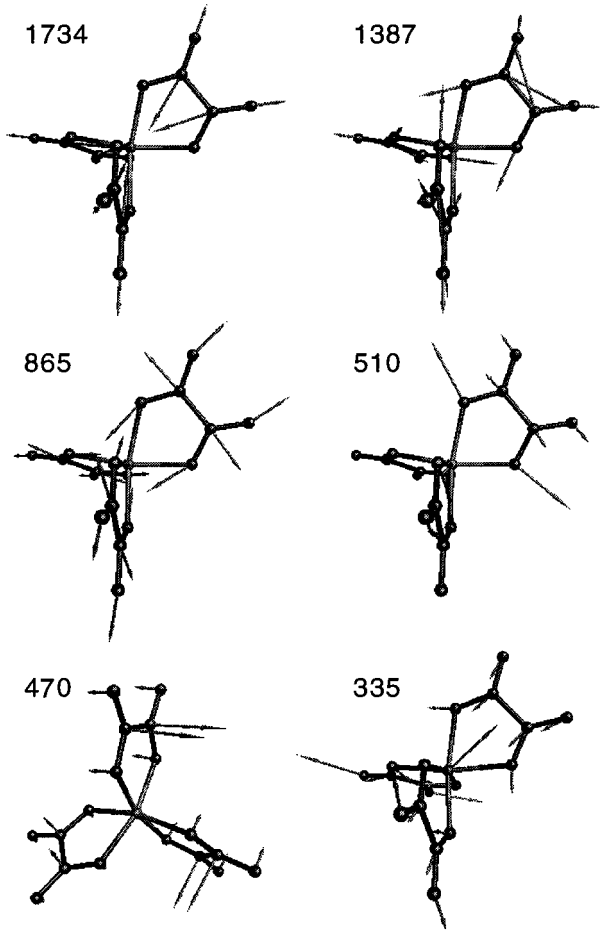

Figure 4. Atomic displacements of selected normal modes for $[Fe(oxalate)_3]^{3-}$ calculated by DFT. The scale of the displacements is arbitrary but common to all the modes.

The Fe(catecholate)$^{2-}$ vibrations deviate in average by 25 cm^{-1} from the closest measured frequencies, and with a maxium deviation of 32 cm^{-1}, the latter figure not surprisingly being associated with the Fe−O bond. For the catecholates substituted in the 4-position, the mean deviation is of the same order. The assignments for the Fe(4-methylcatecholate)$^{2-}$ vibrations correspond approximately to the modes given for Fe(catecholate)$^{2-}$, but because of the methyl group, they are not exactly equivalent.

These deviations are small enough for us to believe that the normal modes are correctly reproduced, and a recent resonance Raman study supports these assignments.[47] This assumption was further checked by model calculations on $[Fe(oxalate)_3]^{3-}$, $Li_3[Fe(oxalate)_3]$, and Fe(oxalate)$^{2-}$ as we report in the following section.

$[Fe(oxalate)_3]^{3-}$, $Li_3[Fe(oxalate)_3]$, and Fe(oxalate)$^{2-}$. In Table 2, the population analysis is shown, and in Table 4, we report geometries obtained at the LSD level and some relevant experimental data.[48,49] Vibrations are reported in Table 5 together with experimentally determined frequencies. Some important normal modes are illustrated in Figure 4.

When we compare $[Fe(oxalate)_3]^{3-}$ and Fe(oxalate)$^{2-}$ vibrations on the LSD level, we see that from 400 cm^{-1} and upward the vibrational modes are the same; each Fe(oxalate)$^{2-}$ vibration normally corresponds to three $[Fe(oxalate)_3]^{3-}$ vibrations, and they come in the same order. If we take the average values of the $[Fe(oxalate)_3]^{3-}$ frequencies, then the mean deviation between the two models is 27 cm^{-1}. This supports our assumption that Fe(0)catecholate models should give vibrational modes close to the vibrations in Fe(III)catecholate complexes. However, it will also be of interest to compare the calculated $[Fe(oxalate)_3]^{3-}$ vibrations to experimental data.

TABLE 4: LSD Optimized Geometries for Fe(oxalate)$^{2-}$, $[Fe(oxalate)_3]^{3-}$, and $Li_3[Fe(oxalate)_3]$ Compared to Some Experimental Data

	LSD[a] [Å] $Fe(ox)^{2-}$	LSD [Å] $Fe(ox)_3^{3-}$	LSD [Å] $Li_3[Fe(ox)_3]$	Exptl[b] [Å] $M_3[Fe(ox)_3]$
C1−O1	1.303	1.289	1.279	1.262−1.282
C1−C2	1.536	1.559	1.571	1.529−1.556
C1−O2	1.248	1.244	1.267	1.214−1.250
Fe−O1	1.860	2.024	2.058	1.979−2.024
Li−O2			1.911	2.193−2.127
O1−Fe−O1	85.5°	78.7°	80.5°	80.5°

[a] The BP calculations gave somewhat longer bond lengths, significantly so for the Fe−O bond (1.932 Å). [b] From ref 48, $Li_3[Fe(ox)_3]LiCl\cdot 9H_2O$, and ref 49, $(NH_4)_3[Fe(ox)_3]\cdot 3H_2O$. These are representative examples, several other structures have been determined.

The $[Fe(oxalate)_3]^{3-}$ unit is highly charged. In solution, charge compensating cations may be close by, although not necessarily forming well-defined ion pairs, and in the solid state, a cation may be coordinated to the oxalate oxygens or the counterions may be packed in some other way in the crystal. We therefore did calculations for both the $[Fe(oxalate)_3]^{3-}$ ion and the neutral model compound $Li_3[Fe(oxalate)_3]$. Somewhat surprisingly, the geometry of the $[Fe(oxalate)_3]^{3-}$ ion comes closer to the experimental values than the $Li_3[Fe(oxalate)_3]$ model (Table 4). The neutral model clearly overestimates the Li−oxalate interaction, and consequently, the Fe−oxalate bonds become too long. Our conclusion is thus that the $[Fe(oxalate)_3]^{3-}$ ion will serve as a good approximation.

A number of IR and Raman studies of the $[Fe(oxalate)_3]^{3-}$ ion have been published,[50−54] with the most elaborate of these being the study by Fujita et al. whose assignments were based on normal coordinate analysis of a Cr(III)oxalate model.[51a] These studies all concern the $K_3[Fe(oxalate)_3]\cdot 3H_2O$ compound, and in the comparison, we have to be aware of solid-state effects such as different symmetries of the molecule and crystal and vibrations of crystal water. For example, the calculations only give one IR frequency in the 1600 cm^{-1} range, whereas there are two observed ones. Some authors assign this band to an additional C═O stretch,[51a,54] whereas others[53] assign it to crystal water vibrations. For the 12 vibrations between 300 and 1700 cm^{-1} where the assignments seem clear, the mean deviation is 24 cm^{-1}.

Fuijita and co-workers also did a normal coordinate analysis of the $[Cr(oxalate)_3]^{3-}$ ion.[51b] The potassium salt if this ion has an IR spectrum that very closely resembles the spectrum of $K_3[Fe(oxalate)_3]\cdot 3H_2O$ down to 450 cm^{-1}.[51a] An important issue was the coupling of vibrations between ligands. While the model with one chromium and one oxalate ion was shown to well represent a $[Cr(NH_3)_4(oxalate)]^-$ ion, that is, the coupling between the NH_3 ligands and the oxalate ligand was negligible, some interaction was found for the $[Cr(oxalate)_3]^{3-}$ ion. Our results essentially support their conclusions; the coupling between C═O, C−C, and C−O stretchings produces near-degenerate frequencies, a splitting of the O−C═O bending by 10 cm^{-1} is observed, and there is also a larger effect on one of the low-frequency Fe−O stretchings.

An experimental spectrum and a simulated spectrum are shown in Figure 5, where a line broadening of 20 cm^{-1} has been applied to the frequencies from the DFT calculations. The intensity of the carbonyl stretching is clearly overestimated, otherwise the same features appear in both spectra.

TABLE 5: Experimental Vibrations for $K_3[Fe(oxalate)_3]\cdot 3H_2O$ Compared to Frequencies (>210 cm^{-1}) Calculated by DFT for $[Fe(oxalate)_3]^{3-}$ and $Fe(oxalate)^{2-}$[e]

$Fe(ox)^{2-}$ (ν/cm^{-1})			$Fe(ox)_3^{3-}$ (ν/cm^{-1})	IR ν/cm^{-1}			assignment[d]
LSD $S=0$	LSD $S=2$	BP $S=0$	LSD $S=5/2$	exptl[a]	exptl[b]	exptl[c]	based on DFT
1704	1697	1641	(1734) 1698, 1696	1712	1712	1723	νC=O sym
1673	1664	1617	1682 (1678, 1677)	1682	1677	1692	νC=O asym
				1647	*1649*	1659	δH_2O[c]
1331	1310	1320	(1386) 1382, 1382	*1390*	1390	1404	νC−C
1267	1260	1227	1297 (1292, 1291)	1270	*1270*	1280	νC−O asym
				1255	1255	1262	νC−O[a,b,c]
891	864	852	(865) 861, 860	*892*	885	906	δO−C=O sym νC−C
795	810	797	(834, 831, 831)			*855*	out-of-plane asym
				803	797	812	δO−C=O[a,b,c]
759	737	738	751 (742, 741)	790	785	793	δO−C=O asym νFe−O
						664	δO−C=O[c]
555	546	543	(553, 552, 551)	*580*	*580*	*593*	δC−C−O
			(523)				δ,νFe−O
548	467	494	510, 508	532	528	538	δ,νFe−O
405	438	426	479, 474, 470	500	498	508	out-of-plane, sym
352	281	310	335, 333, 332	365	366	358	νFe−ox
309	306	315	330, 330	346	*340*		νFe−O
				328			δFe−O + δring[a]
364	245	287	279	217		253	νFe−O
			(211)	*190*		*223*	νFe−O breathing

[a] Reference 54. [b] Reference 51a. [c] Reference 53. [d] Sym or asym refers to the oxalate ligand only. [e] For $Fe(oxalate)_3^{3-}$, signals with relatively weak IR intensities are indicated in parenthesis. Vibrational modes are assigned based on the DFT results. Experimental values in italics indicate that this reference gives an alternative assignment. Note that all descriptions are approximate, especially for lower frequencies. See Figure 4 for a more detailed description of some of the vibrations.

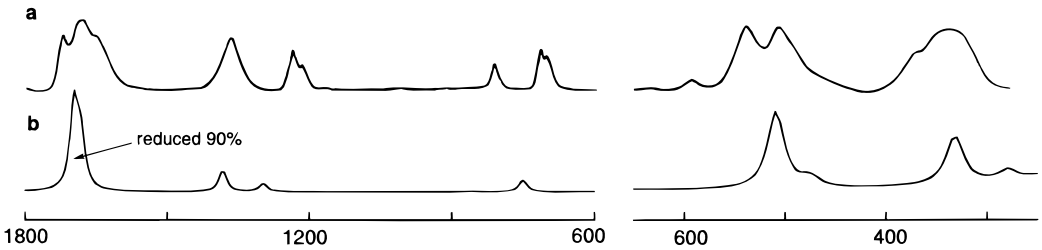

Figure 5. (a) Experimental IR spectrum for $K_3[Fe(oxalate)_3]\cdot 3H_2O$ from ref 51a, compared to (b) a simulated spectrum based on the DFT frequencies and intensities for the $[Fe(oxalate)_3]^{3-}$ ion, Lorenzian peak shape and a 20 cm^{-1} line broadening. The intensities of the theoretical carbonyl strechings have been reduced for clarity. The experimental spectrum reprinted (abstracted) with permission from Fujita, J.; Martell, A. E.; Nakamoto, K. *J. Chem. Phys.* **1962**, *36*, 324. Copyright 1962 American Institute of Physics.

The assembled experimental data lend credibility to the calculations on the $[Fe(oxalate)_3]^{3-}$ ion, however, only within a rather large margin of error, especially when it comes to the assignments. These experimental data need to be complemented with isotopic substitution experiments, and measurements should also be made on samples with different counterions. Only then would it be meaningful to enter into a detailed discussion of each vibrational mode and its assignment.

We also have to see that the LSD level, used for the oxalates, gives comparable results to the BP level of calculation, used for the catecholates. For $Fe(oxalate)^{2-}$, LSD and BP levels of theory give identical vibrational modes above 400 cm^{-1}. For the low-frequency vibrations, some frequencies are (accidentally) very close in energy. This may result in some mixing that makes the three vibrations in the 300 cm^{-1} range somewhat different. Since the low-energy vibrations normally are much more closely spaced than the high-frequency vibrations, this is always a risk and these values have to be treated with caution. The two last vibrations are again identical. The mean deviation between the BP and LSD vibrations is 32 cm^{-1}, and in most cases, the BP frequencies are lower; see Table 5. This is consistent with the "BP bond lengths" being somewhat longer, although there seems to be no general trend when differences in bond lengths and differences in frequencies are compared. It is interesting to note that, for the model compound, the LSD frequencies come closer to experimental values than those calculated by the BP functional.

Finally, we have to consider the different possible spin states for the iron atom. Additional LSD calculations were made for the $S=1$ and $S=2$ states. As expected, the Fe−O bond lengths increase with increasing spin, and the $S=2$ state has an Fe−O distance of 1.96 Å. The $S=2$ state is also the ground state of this hypothetical molecule, lower by 10 kcal/mol. However, the vibrational modes do not change, and the main difference is the expected lowering of all the frequencies involving νFe−O vibrations. The frequencies are reported in Table 5, and it can be noted that the Fe−O vibrations in many cases come closer to those of the $S=0$ BP calculation on $Fe(oxalate)^{2-}$, which gave similar Fe−O bond lengths, than to the $S=0$ LSD calculation. There is, nevertheless, nothing to suggest that the more expensive $S=2$ calculations should be a superior model.

We can now, by analogy, conclude that the calculations for the Fe(0) model compounds should reproduce the experimental vibrational modes for "real" Fe(III)catecholate complexes with a good accuracy, and thus, the prediction of substitution shifts should be possible. The agreement with observed frequencies will be only qualitative, but as we want to compare to a whole class of compounds where the experimental values will differ between complexes anyway (see Figure 3), this is not an obstacle.

TABLE 6: Isotopic Shifts Calculated by DFT for Fe(catecholate)$^{2-}$ and by the Diatomic Harmonic Oscillator (DHO), Compared to Experimental Data for Tyrosine Hydroxylase Fe(III) Complexes with Catecholate and Catecholate Derivatives[f]

		$\Delta\nu(^{54/57}Fe)/cm^{-1}$			$\Delta\nu(^{16/18}O)/cm^{-1}$			$\Delta\nu(H-D)/cm^{-1}$	
vibration mode all A_1	ν/cm^{-1} DFT	DFT	DHO[a]	exptl[b]	DFT	DHO	exptl[b]	DFT	exptl[d]
νCC	1537							27	30
νC−O/7a	1292				15	32[c]	5−9	88	57
νFe−O	583	0.3	4	<1	10	27[a]	12	14	10
									10[e]
δ,ν chelate	489	0.1	3	<1	20	23[a]	18−19	6	6, 4[e]
νFe−cat	283	5	2	na	1	14[a]	na	3	3[e]

[a] Fe−O vibration. [b] From ref 6, average values for noradrenaline and dopamine bound TH. [c] C−O vibration. [d] From ref 6, catecholate bound to TH. [e] From ref 17b [Fe(PDA)catecholate]$^-$. [f] Isotopic substitutions have been performed with $^{16/18}O$, $^{54/57}Fe$, and H/D.

TABLE 7: Isotopic Shifts Calculated by DFT and by the Diatomic Harmonic Oscillator (DHO) for Mono- and Di-^{18}O-substituted Fe(4-methylcatecholate)$^{2-}$ Compared to Experimental Data for Dopamine Bound to Tyrosine Hydroxylase and 3,4-Dihydroxyphenylacetate Bound to Protocatechuate 3,4-Dioxygenase

		$\Delta\nu(^{16/18}O)/cm^{-1}$						
		$(2-^{18}O,1-^{18}O)$			$(2-^{18}O,1-^{16}O)$		$(2-^{16}O,1-^{18}O)$	
vibration	DFT ν/cm^{-1}	DFT	DHO[a]	exptl[b]	DFT	exptl[b,c]	DFT	exptl[c]
νC−O/7a	1293	13	32	9	5	4		
νFe−O	625	14	29	12	3	2, 0	11	10
νFe−O	552	16	29	14	16	12, 10	0	0
δ,ν-chelate	500	21	24	19	9	6, 6	13	8
νFe-cat	282	1	13					

[a] C−O or Fe−O vibrations. [b] Dopamine bound to TH, ref 6. [c] 3,4-Dihydroxyphenylacetate bound to protocatechuate 3,4-dioxygenase, ref 55b.

Isotopic Shifts. Isotopic shifts are important for the analysis of complex spectra from, for example, metalloproteins. These shifts are very dependent on the mixing of different components in the vibrational mode, for example νCC with νCO, and there is obviously molecular information imbedded in these values.

To extract these values by normal coordinate analysis may prove very difficult for complicated systems. An alternative approach is therefore to calculate the vibrational frequencies and shifts with some quantum chemistry method. This has, furthermore, a certain appeal since the method is completely independent from the experimental data, in contrast to normal coordinate analysis.

In our preliminary communication,[16] we showed how the $^{16/18}O$, $^{54/57}Fe$, and $^{1/2}H$ isotopic substitution shifts obtained for the model compound Fe(catecholate)$^{2-}$ using DFT matched the experimental pattern for the resonance Raman study of tyrosine hydroxylase with catecholate derivatives.[6] The calculated and experimental isotopic substitution shifts for Fe(catecholate)$^{2-}$ and Fe(4-methylcatecholate)$^{2-}$ can be found in Tables 6 and 7. It is clear that extensive mixing with the aromatic ring occurs for the vibrations involving oxygen and that this leads to discrepancies of up to 60% when the diatomic harmonic oscillator model is used to interpret the isotopic shifts for oxygen-18 substitution. For iron isotopes, the discrepancies are even worse, up to 90%; see Table 6.

For the 4-substituted catecholate complex, our calculations correctly predict the difference in isotope effect between the different Fe−O vibrations for the ^{18}O-mono- and di-substituted dopamine−TH complex and the ^{18}O-monosubstituted 3,4-dihydroxyphenylacetate(HPCA) bound to protocatechuate 3,4-dioxygenase(3,4-PCD);[55b] see Table 7. Since one weaker Fe−O bond is implicated in the subsequent reaction of the catecholate with dioxygen catalyzed by dioxygenases,[55] the identification of such a bond by vibrational spectroscopy may be a significant help in mechanistic studies.

The calculations also provided an explanation for the puzzling absence of any $^{54}Fe/^{57}Fe$ effect in the tyrosine hydroxylase study.[6] It appeared that there should indeed be such an effect of the order of 5 cm^{-1} but only for the newly assigned νFe−O band predicted at 305−330 cm^{-1} in an experimental spectrum (calculated at 283 cm^{-1}), thus outside the spectral window used in ref 6. As may be seen in Figure 2, this vibration corresponds to a movement of the entire (rigid) catecholate ligand, and there are also corresponding [Fe(oxalate)$_3$]$^{3-}$ vibrations; see Figure 4. Consequently,we would like to label these vibrations νFe−cat and νFe−ox.

Although the calculations are less reliable for lower frequencies, we also note the good agreement of the calculated H/D isotope effect for the 283 cm^{-1} mode, 3 cm^{-1}, with the experimental shift of the 310 cm^{-1} peak in the spectra of [Fe(PDA)catecholate]$^-$, 3 cm^{-1}.[17b] The $^{54}Fe/^{57}Fe$ shift of 0.3 cm^{-1} for the 583 cm^{-1} vibration of Fe(catecholate)$^{2-}$ is furthermore in good agreement with the shift of 0.7 cm^{-1} observed for the [Fe(salen)(*p*-cresolate)] frequency at 570 cm^{-1}, given the experimental difficulties when measuring such small shifts.[56]

Correspondingly, for [Fe(oxalate)$_3$]$^{3-}$, no $^{54}Fe/^{57}Fe$ isotopic shifts larger than 0.5 cm^{-1} were found for frequencies over 400 cm^{-1}. (The Fe−oxalate isotopic shifts are only reported here and are not included in the tables.) For the νFe−O vibrations around 350 cm^{-1}, shifts of 2−4 cm^{-1} were found. For a completely ^{18}O-substituted species, the νC═O vibrations have isotopic shifts of 30 and 26 cm^{-1}, considerably lower than those predicted by the diatomic harmonic oscillator model (DHO), 41 and 40 cm^{-1}. The νC−O vibrations have higher shifts, 38 cm^{-1}, than that predicted by DHO, 31 cm^{-1}, and there is notably a significant effect on the νC−C vibrations, 28 cm^{-1}, as well. The δO═C−O vibrations also show significant isotope effects in the DFT calculations, 32−34 cm^{-1}. The νFe−O ^{18}O shifts fall very close to those predicted by DHO, 26 cm^{-1} versus 23−24 cm^{-1} for the vibrations around 500 and 17 cm^{-1} versus 15 cm^{-1} for the 300 cm^{-1} vibrations.

We note that, in line with intuition, the DHO model is significantly better suited to interpret the isotopic shifts for the simpler oxalato complex. Here, for the vibrations assigned to pure stretching modes, the difference between DFT and the DHO model is normally less than 30%, often better. However, the large differences for $^{54}Fe/^{57}Fe$ effects remain.

Concluding Remarks

DFT calculations on the model compounds Fe(catecholate)$^{2-}$ and Fe(4-methylcatecholate)$^{2-}$ give reasonable vibrational frequencies and predict isotope shifts that are in good agreement with experimental data. Clear assignments of the vibration modes are also obtained that allow us to confirm previous hypotheses of, for example, a "chelate" vibration mode.

Comparison between [Fe(oxalate)$_3$]$^{3-}$ and Fe(oxalate)$^{2-}$ vibrations validates further the use of a simple Fe(0) model compound. For these two complexes, the vibration modes are identical down to 400 cm^{-1}. Clearly low-frequency modes demand additional attention; for example, it is only in this regime that we encounter near degeneracy between different vibration modes, and that may be a complication.

The utility of the resonance Raman isotopic labeling spectroscopy may be enhanced by this method since we will have a more precise tool when interpreting the data. Especially interesting are the possibilities to model different possible structures, for example, reaction intermediates in metallobiochemistry, and then match the experimental isotopic shift pattern to the different calculated alternatives.

While we are satisfied with the qualitative agreement of the calculated frequencies and the quantitative prediction of isotopic substitution shifts in this study, we finally have to add that to take this a step further and quantitatively predict vibrational frequencies for coordination complexes, in solution or imbedded in a protein, will be more demanding.

Acknowledgment. We thank the Commissariat à l'Energie Atomique for the use of the CRAY-C94 supercomputer in Grenoble, Dr. J-M Latour, CEA-Grenoble, and Prof. L. Que, Jr., University of Minnesota, for valuable discussions. L.Ö. is grateful to the Swedish Research Council for Engineering Sciences for funding.

References and Notes

(1) Frushour, B. G.; Koenig, J. L. In *Advances in Infrared and Raman Spectroscopy*; Clark, R. J. H., Hester, R. E., Eds.; Heyden: London, 1975; Vol. 1, p 35. In the DHO-model the frequency shift for two vibrating atoms is calculated according to Hook's law as $\nu_h = \nu_l(\mu_l/\mu_h)^{0.5}$ where index h or l indicates heavy or light isotopes and μ is the reduced mass.

(2) Spiro, T. G.; Czernuszewicz, R. S. In *Methods in Enzymology*; Academic Press: New York, 1995; Vol. 246, p 416.

(3) Loehr, T. M.; Sanders-Loehr, J. In *Methods in Enzymology*; Academic Press: New York, 1993; Vol. 226, p 431.

(4) Andrew, C. R.; Yeom, H.; Valentine, J. S.; Karlsson, B. G.; Bonander, N.; Pouderoyen, G. v.; Canters, G. W.; Loehr, T. M.; Sanders-Loehr, J. *J. Am. Chem. Soc.* **1994**, *116*, 11489.

(5) Ling, J.; Nestor, L. P.; Czernuszewicz, R. S.; Spiro, T. G.; Fraczkiewicz, R.; Sharma, K. D.; Loehr, T. M.; Sanders-Loehr, J. *J. Am. Chem. Soc.* **1994**, *116*, 7682.

(6) Michaud-Soret, I.; Andersson, K. K.; Que, L., Jr.; Haavik, J. *Biochemistry* **1995**, *34*, 5504.

(7) Nakamura, N.; Matsuzaki, R.; Choi, Y. H.; Tanizawa, K.; Sanders-Loehr, J. *J. Biol. Chem.* **1996**, *271*, 4718.

(8) Takahashi, S.; Ishikawa, K.; Takeuchi, N.; Ikeda-Saito, M.; Yoshida, T.; Rousseau, D. L. *J. Am. Chem. Soc.* **1995**, *117*, 6002.

(9) For example, see: Zhou, X.; Wheeless, C. J. M.; Liu, R. *Vib. Spectrosc.* **1996**, *12*, 53.

(10) Fan, L.; Ziegler, T. *J. Chem. Phys.* **1992**, *96*, 9005.

(11) Abbreviations are as follows: DFT, density functional theory; LSD, local spin density; VWN, Vosko−Wilk−Nusair; BP, Becke−Perdew nonlocal corrections to the exchange energy; RHF, restricted Hartree−Fock; UHF, unrestricted Hartree−Fock; DZVP, double-ζ split-valence plus polarization; cat, catecholate; 4mecat, 4-methyl-catecholate; PDA, *N*-(2-pyridylmethyl)-*N*-(carboxymethyl)glycinate; NTB, *N*-tris(2-benzimidazolylmethyl)amine, DOPA, 3-(3,4)-dihydroxyphenyl)-alanine; DHBN, 3,4-dihydroxybenzonitrile, TH, tyrosine hydroxylase; DHO, diatomic harmonic oscillator; 1,2-CTD, catechol 1,2-dioxygenase; ox, oxalate.

(12) (a) Cundari, T. R.; Raby, P. D. *J. Phys. Chem. A* **1997**, *101*, 5783 and references therein. (b) Papai, I.; Mink, J.; Fournier, R.; Salahub, D. R. *J. Phys. Chem.* **1993**, *97*, 9986.

(13) Casteel, W. J. J.; Dixon, D. A.; Mercier, H. P. A.; Schrobilgen, G. J. *Inorg. Chem.* **1996**, *35*, 4310.

(14) Bridgeman, A. J. *J. Chem. Soc., Dalton Trans.* **1996**, 2601.

(15) Jacobsen, H.; Ziegler, T. *J. Am. Chem. Soc.* **1996**, *118*, 4631.

(16) Öhrström, L.; Michaud-Soret, I. *J. Am. Chem. Soc.* **1996**, *118*, 3283.

(17) (a) Cox, D. D.; Benkovic, S. J.; Bloom, L.; Bradley, F. C.; Nelson, M. J.; Que, L., Jr.; Wallick, D. E. *J. Am. Chem. Soc.* **1988**, *110*, 2026. The complexes referred to in Figure 3 are Fe(*N*-tris(2-benzimidazolylmethyl)-amine)(cat)$^+$, Fe(bis-*N*-(2-pyridylmethyl)glycinate)(cat)$^+$, Fe(*N*-(2-pyridylmethyl)-*N*-(carboxymethyl)glycinate)(cat)$^-$, Fe(nitrilotriacetate)(cat)$^{2-}$, Fe(bis(salicylidene)ethylenediamino)(cat)$^-$, and Fe(cat)$_3^{3-}$. (b) Cox, D. D. Ph.D. Thesis, University of Minnesota, Minneapolis, 1988.

(18) Tyson, C. A. *J. Biol. Chem.* **1975**, *250*, 1765.

(19) Kemal, C.; Louis-Flamberg, P.; Krupinski-Olsen, R.; Shorter, A. L. *Biochemistry* **1987**, *26*, 7064.

(20) Nelson, M. J. *Biochemistry* **1988**, *27*, 4273.

(21) Que, L., Jr.; Lauffer, R. B.; Heistand, R. H., II. In *The coordination chemistry of metalloenzymes*; Bertini, I., Drago, R. S., Luchinat, C., Eds.; D. Riedel Publishing Company: Dordrecht, 1983; p 265.

(22) Siu, D. C.-T.; Orville, A. M.; Lipscomb, J. D.; Ohlendorf, D. H.; Que, L., Jr. *Biochemistry* **1992**, *31*, 10443.

(23) Andersson, K. K.; Cox, D. D.; Que, L., Jr.; Flatmark, T.; Haavik, J. *J. Biol. Chem.* **1988**, *263*, 18621.

(24) Andersson, K. K.; Vassort, C.; Brennan, B.; Que, L., Jr.; Haavik, J.; Flatmark, T.; Gros, F.; Thibault, J. *Biochem. J.* **1992**, *284*, 687.

(25) Nelson, M. J.; Brennan, B. A.; Chase, D. B.; Cowling, R. A.; Grove, G. N.; Scarrow, R. C. *Biochemistry* **1995**, *34*, 15219. The three complexes referred to in Figure 3 are Fe(*N*-tris(2-benzimidazolylmethyl)amine)(4-R-cat)$^+$, where 4-R-cat is the dianion of 3,4-dihydroxybenzonitrile, 3,4-dihydroxybenzaldehyde, and 3,4-dihydroxyacetophenone, respectively.

(26) Taylor, S. W.; Chase, D. B.; Emptage, M. H.; Nelson, M. J.; Waite, J. H. *Inorg. Chem.* **1996**, *35*, 7572.

(27) Andzelm, J.; Wimmer, E. *J. Chem. Phys.* **1992**, *96*, 1280.

(28) *UniChem*, versions 2.3, 3.0, 4.0; Oxford Molecular Group PLC: Oxford OX4 4GA, U. K., 1994−1997.

(29) (a) Vosko, S. H.; Wilk, L.; Nusair, M. *Can. J. Phys.* **1980**, *58*, 1200. (b) Becke, A. D. *Phys. Rev. A* **1988**, *38*, 3098. (c) Perdew, J. P. *Phys. Rev. B* **1986**, *33*, 8822.

(30) For a discussion of DFT calculations of vibrational frequencies, see for example the following: (a) Scott, A. P.; Radom, L. *J. Phys. Chem.* **1996**, *100*, 16502. (b) Pulay, P. *J. Mol. Struct.* **1995**, *347*, 293.

(31) Godbout, N.; Salahub, D. R.; Andzelm, J.; Wimmer, E. *Can. J. Chem.* **1992**, *70*, 560.

(32) For a comparison of small molecules and Fe(0) in different spin states, see also: Ricca, A.; Bauschlicher, C. W. J. *Theor. Chim. Acta* **1995**, *92*, 123.

(33) Nicholls, D. *The Chemistry of Iron, Cobalt and Nickel*; Pergamon Press: Oxford, 1975.

(34) (a) Wunderlich, V. H.; Mootz, D. *Acta Crystallogr.* **1971**, *B27*, 1684. (b) Caminati, W.; Bernardo, d. S.; Schäfer, L.; Kulp-Newton, S. Q.; Siam, K. *J. Mol. Struct.* **1990**, *240*, 263.

(35) Varsanyi, G. D. *Vibrational Spectra of Benzene Derivatives*; Academic Press: New York, 1969.

(36) Varsanyi, G. D. *Assignments for vibrational spectra of seven hundred benzene derivatives*; John Wiley & Sons: New York, 1974; Vol. 1.

(37) (a) Wilson, H. W. *Spectrochim. Acta* **1974**, *30A*, 2141. (b) Greaves, S. J.; Griffith, W. P. *Spectrochim. Acta* **1991**, *47A*, 133.

(38) (a) Ramíres, F. J.; Lopez Navarette, J. T. *Vib. Spectrosc.* **1993**, *4*, 321. (b) Ramíres, F. J.; Lopez Navarette, J. T. *J. Mol. Struct.* **1993**, *293*, 59. (c) Lopez Navarette, J. T.; Ramíres, F. J. *Spectrochim. Acta* **1993**, *49A*, 1759.

(39) Qin, Y.; Wheeler, R. A. *J. Chem. Phys.* **1995**, *102*, 1689.

(40) Qin, Y.; Wheeler, R. A. *J. Am. Chem. Soc.* **1995**, *117*, 6083.

(41) Zerovalent transition metals with one or two ligands have been used extensively by Siegbahn, Blomberg, and co-workers in model studies of organometallic reaction mechanisms and energetics. Blomberg, M. R. A.; Siegbahn, P. E. M.; Svensson, M.; Wennerberg, J. In *Energetics of Organometallic Species*; Martinho Simões, J. A., Ed.; Kluwer Academic Publishers: Netherlands, 1992; pp 387−421. Also, for example, see: Siegbahn, P. E. M. *J. Am. Chem. Soc.* **1994**, *116*, 7722. It was concluded that many trends seen across the transition metal rows in the periodic table can be understood from the properties of these models but that also ligand effects may be significant.

(42) Raymond, K. N.; Isied, S. S.; Brown, L. D.; Fronczek, F. R.; Nibert, J. N. *J. Am. Chem. Soc.* **1976**, *98*, 1767.

(43) Andersson, B. F.; Buckingham, D. A.; Robertson, G. B.; Webb, J. *Acta Crystallogr. B* **1982**, *38*, 1927.

(44) Lauffer, R. B.; Heistand, R. H., II.; Que, L., Jr. *Inorg. Chem.* **1983**, *22*, 50.

(45) Koch, W. O.; Kruger, H. J. *Angew. Chem., Int. Ed. Engl.* **1996**, *34*, 2671.
(46) Grillo, V. A.; Hanson, G. R.; Wang, D. M.; Hambley, T. W.; Gahan, L. R.; Murray, K. S.; Moubaraki, B.; Hawkins, C. J. *Inorg. Chem.* **1996**, *35*, 3568.
(47) Hartl, F.; Barbaro, P.; Bell, I. M.; Clark, R. J. H.; Snoeck, T. L.; Vlcek, A., Jr. *Inorg. Chim. Acta* **1996**, *252*, 157.
(48) Declercq, J. P.; Feneau-Dupont, J.; Ladriere, J. *Polyhedron* **1993**, *12*, 1031.
(49) Merrachi, E. H.; Mentzen, B. F.; Chassagneux, F.; Bouix, J. *Rev. Chim. Miner.* **1987**, *24*, 56.
(50) Schmelz, M. J.; Miyazawa, T.; Mizushima, S.-i.; Lane, T. J.; Quagliano, J. V. *Spectrochim. Acta* **1957**, *9*, 51.
(51) (a) Fujita, J.; Martell, A. E.; Nakamoto, K. *J. Chem. Phys.* **1962**, *36*, 324. (b) Fujita, J.; Martell, A. E.; Nakamoto, K. *J. Chem. Phys.* **1962**, *36*, 331.
(52) Vaisserman, J.; Lucas, M. R. *Compt. Rend. Acad. Sci. Paris, B* **1970**, *270*, 948.
(53) Homborg, H.; Preetz, W. *Spectrochim. Acta* **1976**, *32A*, 709.
(54) Gouteron, J. *J. Inorg. Nucl. Chem.* **1976**, *38*, 55.
(55) (a) Lipscomb, J. D.; Orville, A. M. In *Metal Ions in Biological Systems*; Siegel, H., Siegel, A., Eds.; Marcel Dekker: New York, 1992; Vol. 28, p 243. (b) Elgren, T. E.; Orville, A. M.; Kelly, K. A.; Lipscomb, J. D.; Ohlendorf, D. H.; Que, L. *Biochemistry* **1997**, *36*, 11504.
(56) Pyrz, J. W.; Roe, A. L.; Stern, L. J.; Que, L., Jr. *J. Am. Chem. Soc.* **1985**, *107*, 614.